# Apoptosis and Necrosis are Involved in the Toxicity of *Sauropus androgynus* in an *In Vitro* Study

*Shih-Fing Yu,[1] Tzer-Ming Chen,[2] Yen-Hui Chen[1,3]**

**Background/Purpose:** The raw juice of the young sticks and leaves of *Sauropus androgynus* (SA) has been widely used as a natural food for body weight reduction and vision protection in Taiwan and Southeast Asia. But as has been reported, SA-associated obliterative bronchiolitis can develop after taking SA for more than 3 months. Lung transplantation was carried out in severe cases.

**Methods:** To study the toxic effect, we separated the SA extract into three parts, namely $CHCl_3$, EtOAc and n-BuOH fractions, using polarity dissection. NIH3T3 fibroblasts were treated with the SA fractions 300 μg/mL and subjected to a series of cytotoxic assays.

**Results:** The EtOAc fraction exhibited the strongest effect of cell growth inhibition, followed by the $CHCl_3$ and n-BuOH fractions. Features of condensed chromatin and apoptosis were observed in cells exposed to n-BuOH and EtOAc fractions using fluorescence microscopy. Formation of DNA ladders was also observed in the above cells. Instead, the $CHCl_3$ fraction induced DNA smearing. In bivariate dot plots of annexin V and propidium iodide double staining, necrosis and apoptosis appeared in cells treated with $CHCl_3$ and n-BuOH fractions, respectively, and a mixed type of necrosis and apoptosis appeared in EtOAc fraction-treated cells.

**Conclusion:** Our results indicate that necrosis and apoptosis are involved in the toxic effect of SA in NIH3T3 fibroblasts. More evidence is needed to clarify if necrosis and apoptosis are also related to the pathogenesis of SA-associated obliterative bronchiolitis. [*J Formos Med Assoc* 2007;106(7):537–547]

**Key Words:** apoptosis, lung obstruction, necrosis, *Sauropus androgynus*

*Sauropus androgynus* (SA), a member of the euphorbiaceae family, has been consumed as a highly nutritious food, widely distributed in high-temperature and humid regions like Malaysia, Indonesia, Southwest China and Vietnam. It is recorded as a tropical vegetable by the United States Department of Agriculture.[1] It is a cheap source of dietary proteins and has earned the name of *multigreen* for its high vitamin content.[2,3] Chemical constituents from SA extract have been identified, such as lignans including (+)-isolariciresinol 3α-*O*-β-glucopyranoside, (−)-isolariciresinol 3α-*O*-β-glucopyranoside, (+)-syringaresinol and di-*O*-β-glucopyranoside; megastigamans; nucleosides; and flavonol glucosides including two diosides: 3-*O*-β-D-glucosyl-7-*O*-α-L-rhamnosyl-kaempferol and 3-*O*-β-D-glucosyl-(1 → 6)-β-D-glucosyl-kaempferol, and one rare trioside: 3-*O*-β-D-glucosyl-(1 → 6)-β-D-glucosyl-7-*O*-α-L-rhamnosyl-kaempferol.[4,5]

An outbreak of obstructive pulmonary disease occurred in people who had heavily consumed the raw juice of SA over a long period in Taiwan.[6–8]



[1]Institute of Pharmaceutical Sciences and [3]Institute of Clinical Pharmacy, College of Medicine, National Taiwan University, and [2]Department of Obstetrics/Gynecology, National Taiwan University Hospital, Taipei, Taiwan.

**Received:** January 18, 2007
**Revised:** January 31, 2007
**Accepted:** March 13, 2007

***Correspondence to:** Dr Yen-Hui Chen, Institute of Pharmaceutical Sciences, College of Medicine, National Taiwan University, 1, Section 1, Jen-Ai Road, Taipei 100, Taiwan.
E-mail: tcyhchen@ntu.edu.tw

In 60.7% of 178 intoxicated patients, they had generally consumed up to 150 g of SA on a daily basis as raw juice for various periods of time.[9] After cumulative ingestion of more than 3000 g of SA, obstructive ventilatory defects developed in 40% of the patients.[10] In some cases, less than 1200 g of accumulative SA consumption evoked symptoms in patients. The patients still suffered from difficulty in breathing even after ceasing consumption over a long period of time. Although there were some cases of mortality, most patients developed chronic respiratory failure. These pathologic changes are most likely to be related to segmental ischemic necrosis of the bronchi at the water-shed zone of bronchial and pulmonary circulation.[11] The necrotic zone indicates fibrosis and atrophy of cartilage, fibroblasts, and smooth muscle cells.

Necrosis is regarded as a passive response to extremes of environmental stimuli, such as heat and ultraviolet light, and is characterized by cytoplasmic swelling, rapid loss of plasma membrane integrity, and cell lysis.[12] It has been documented that the mode of cell death may be dependent on the cell type, the concentration of stimulus employed, and its environmental setting.[13] Apoptosis, however, is a well-defined programmed response that results in morphologic and biochemical changes, such as cell shrinkage and condensation and fragmentation of nuclear materials.[14]

Under pathologic conditions, apoptosis and necrosis may often coexist *in vivo*.[15] Molecular switches between apoptosis and necrosis include adenosine triphosphate-dependent steps in the activation of caspases or steps sensitive to reactive oxygen/nitrogen species.[16] There are more than six factors identified to switch the death pathway between necrosis and apoptosis. (1) High levels of ATP enable cells to undergo apoptosis, while low ATP levels shift cell death toward necrosis.[17,18] (2) Fibroblasts from PARP-1 deficient mice are protected from ATP depletion and necrosis but not from apoptotic cell death.[19] (3) Mitochondria permeability transition (MPT) is the common factor in ischemia/reperfusion that initiates both apoptotic and necrotic cell killing.[20] (4) Removal of $Ca^{2+}$ from medium protects cells from necrosis induced by starvation and anoxia.[21] (5) Oxidized sterols induce necrosis in fibroblasts, but apoptosis in endothelial and smooth muscle cells.[22] (6) In mice, without Apaf-1 or caspase-3/caspase-9, apoptotic cell death during development switches to necrosis.[23] In addition, flow cytometric identification and quantification of apoptotic or necrotic cells are based on the analysis of a particular biochemical or molecular feature that is characteristic for either necrosis or apoptosis.[24,25]

Studies of SA have been focused on the toxicity in clinical use and pathologic biopsy of the lung. To date, there have been few studies on the identification of the major components and their mechanisms involved in obstructive lung disease. In the present study, we separated the SA extract into three fractions by polarity dissection. According to a previous report, the components in the $CHCl_3$ fraction are non-polar and lipid soluble; components in the EtOAc fraction are less polar; and components in the n-BuOH fraction are polar, containing some flavonol glucosides.[5] Fibroblastic NIH3T3 cells were employed to investigate the characteristics of the partial purified SA fractions *in vitro*. The intoxication mechanism at the cellular level was studied using a series of cytotoxic assays. The various deleterious effects of the fractionized SA extract may be attributed by the unidentified components in different fractions of SA. In the experiments, we demonstrated that necrosis, apoptosis and a mixed type appeared in NIH3T3 cells treated with $CHCl_3$, n-BuOH and EtOAc fractions of SA extract, respectively.

## Methods

### *Cell culture*

NIH3T3 cells were cultivated in Dulbecco's modified Eagle's medium (DMEM) supplemented with 10% fetal bovine serum and 1% penicillin/streptomycin (10,000 U penicillin/mL and 10 mg/mL streptomycin) at 37°C/5% $CO_2$. The experimental medium was changed with 4%

fetal bovine serum, and then treated with camptothecin (Sigma Chemical Co., St Louis, MO, USA) or the SA extract.

### *SA extract preparation*

The fresh aerial young leaves and stalks (6.5 kg) of *S. androgynus* (L.) Merr were harvested from Southern Taiwan and mixed with 95% EtOH for 3 days. After centrifugation and evaporation, an oily residue (309 g) was obtained. The EtOH extract was sequentially fractionized into $CHCl_3$, EtOAc and n-BuOH fractions,[5] followed by concentration and evaporation to dryness in vacuum. Yields of three fractions were 83 g ($CHCl_3$ soluble), 1.42 g (EtOAc soluble) and 7.95 g (n-BuOH soluble). Organic solvent-insoluble fraction was the leftover in the extraction procedure.

### *MTT assay*

Cells were plated at a density of $1.5 \times 10^3$ cells/well into 96-well plates, treated with SA fractions for 0–72 hours, followed by incubation with MTT dye for 4 hours.[26] The supernatant was removed, and DMSO was added to dissolve the resulting formazan residue. Formation of formazan was detected by optical density at 570 nm using a $V_{max}$ Microtiter Plate Reader (ELX800; Bio-Tek Instruments Inc., Winooski, VT, USA).

### *Cell cycle analysis*

NIH3T3 cells grew in 10 $cm^2$ dishes to 70–90% confluence, incubated with fresh medium containing SA fractions for 0–72 hours. Cells were harvested and the supernatant medium was included in the analysis. Cells were fixed in 100% ice-cold ethanol and were stored at −20°C overnight. Fixed cells were treated with 1 mL of phosphate-buffered saline (PBS) buffer containing 0.5% Triton X-100 and 0.5 μg/mL RNase A for 30 minutes, then added with 1 mL of 50 μg/mL propidium iodide (PI in PBS) for 30 minutes at room temperature. Nuclei were stained, illuminated as DNA-PI fluorescence, detected by Becton Dickinson FACScan flow cytometry at 488 nm for excitation and through a 585/42 band pass filter for emission.[27] Ten thousand events were collected from each sample. CELLQuest software, version 3.1 (Becton Dickinson, Franklin Lakes, NJ, USA), was used for data acquisition.

### *Cytochemical staining*

The cover slip was placed on a 60 mm petri dish, and then cells ($2 \times 10^6$) were seeded. After 24 hours, 10% fetal bovine serum in DMEM was reduced to 4%. Cells were harvested after treatment with SA fractions for 0–72 hours. The medium was removed from the dish, and the monolayer was washed twice with PBS. Two milliliters of 25% glacial acetate and 75% methanol were added and incubated for 10 minutes at room temperature. The cell monolayer was washed a further three times, added to 1 mL of Hochest dye solution and incubated at room temperature in the dark for 10 minutes, followed by three courses of washings with distilled water. Blue fluorescence was detected between excites at 360 nm and emits at 490 nm using a Nikon microscope. Brightly stained condensed chromatin was detected in apoptotic cells.

### *DNA fragmentation*

NIH3T3 cells ($5 \times 10^5$ cells/mL) were harvested, washed by PBS, and then lysed by a digestion buffer containing 0.5% sarkosyl, 0.5% mg/mL proteinase K, 50 mM Tris (hydroxymethyl) aminomethane (pH 8.0), 10 mM EDTA at 56°C for 3 hours and treated with RNase A (0.5 μg/mL) for another 2 hours at 56°C. The DNA was extracted by phenol/chloroform/isoamyl (25/24/1) before loading and analyzed by 1.5% agarose gel electrophoresis. The agarose gels were run at 50 volts for 120 minutes in TAE (Tris-borate/EDTA electrophoresis buffer). Approximately 20 μg of DNA was loaded into each well and visualized under UV light and photographed.

### *Flow cytometry and annexin V/PI analysis*

FITC-annexin V/PI-double staining of PS and cellular DNA was performed as described.[28] After washing with PBS, $2 \times 10^6$ cells were resuspended in 100 μL of annexin V/PI solution. The mixture was incubated for 15 minutes in the dark on ice and

was then analyzed by flow cytometry in a manner similar to that used for cell cycle analysis.[29,30]

### *Statistical analysis*

Data are expressed as mean ± standard deviation unless otherwise specified. Student's *t* test was used to analyze individual differences.

## Results

### *SA fractions cause a dose- and time-dependent decrease in cell survival*

SA extract was fractionized into three parts including $CHCl_3$, EtOAc and n-BuOH fractions by polarity dissection (Figure 1). Fibroblastic NIH3T3 cells were introduced as an *in vitro* model to investigate the characteristic of partial purified SA fractions. NIH3T3 cells were treated with 100–300 μg/mL of SA fractions for 0–48 hours. The number of live cells was determined by MTT assays. Inhibition of cell viability was concentration-dependent (Figure 2). The $IC_{50}$ of n-BuOH and $CHCl_3$ fractions was 144 μg/mL and 58 μg/mL, respectively. EtOAc fraction exerted an $IC_{50}$ as low as 13 μg/mL. Three hundred micrograms per milliliter of SA fractions caused potent inhibition of NIH3T3 cell viability. In the time-dependent study, viability of NIH3T3 cells was < 6% of control after cells were exposed to EtOAc fraction for 48 hours (Figure 3). The EtOAc fraction appeared to be the most lethal over $CHCl_3$ and n-BuOH fractions. The n-BuOH fraction only inhibited 14% of cell growth after 24 hours of incubation while presenting a 69% inhibition after 48 hours of incubation. The $CHCl_3$ fraction inhibited 41% of cell growth at 24 hours, while a 77% inhibition was observed at 48 hours. However, the cytotoxicity of the $CHCl_3$ fraction decreased when the fraction was stored at 4°C for 1 week. It may be due to the unstable ingredients in the fraction, resulting in attenuation of the activity.

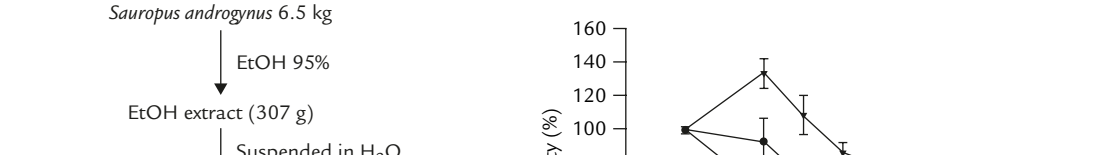


**Figure 1.** Extraction and isolation of *Sauropus androgynus* (SA). The fresh aerial part (6.5 kg) of *S. androgynus* (L.) Merr. was ground portion wise with 95% EtOH by a 5 L-blender, and the supernatant was collected after centrifugation. The EtOH extract (307 g) was resuspended in 1 L of water and successively partitioned with $CHCl_3$, EtOAc and n-BuOH to yield fractions.

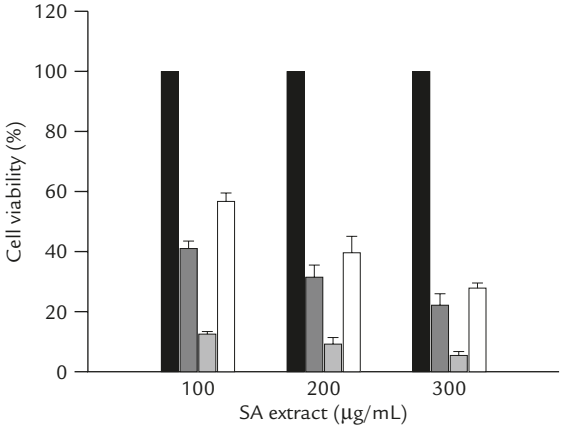


**Figure 2.** Concentration-dependent effect of *Sauropus androgynus* (SA) extract on NIH3T3 cell viability. Control (■), $CHCl_3$ (■), EtOAc (■) and n-BuOH (□) fractions of SA extract (100–300 μg/mL) were added to NIH3T3 cells for 48 hours. Cell viability was detected by the MTT assay. Data are presented as mean ± standard error for six determinations.

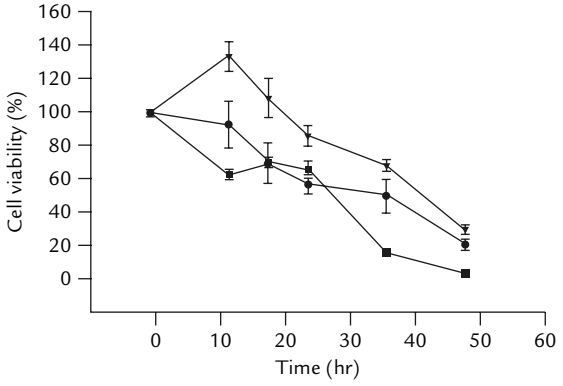


**Figure 3.** Cytotoxicity of *Sauropus androgynus* (SA) extracts. NIH3T3 cells were treated with 300 μg/mL of $CHCl_3$ (●), EtOAc (■) and n-BuOH (▼) fractions of SA extract for 0–48 hours. Cell viability was detected by the MTT assay. Data are presented as mean ± standard error for six determinations.

### *Effect of SA fractions on cell cycle*

Flow cytometric analysis showed that NIH3T3 cells underwent $G_1$, S and $G_2$ progression and were affected when cells were treated with different fractions of SA extract for certain amounts of time (Figure 4). Cells incubated with $CHCl_3$, EtOAc and n-BuOH fractions of 300 μg/mL, respectively, for 24 hours caused different levels of accumulation of PI fluorescence in the sub-$G_1$ population. Deficits of DNA content in apoptotic cells were often recognized by the appearance of the sub-$G_1$ phase on DNA content histograms when cells

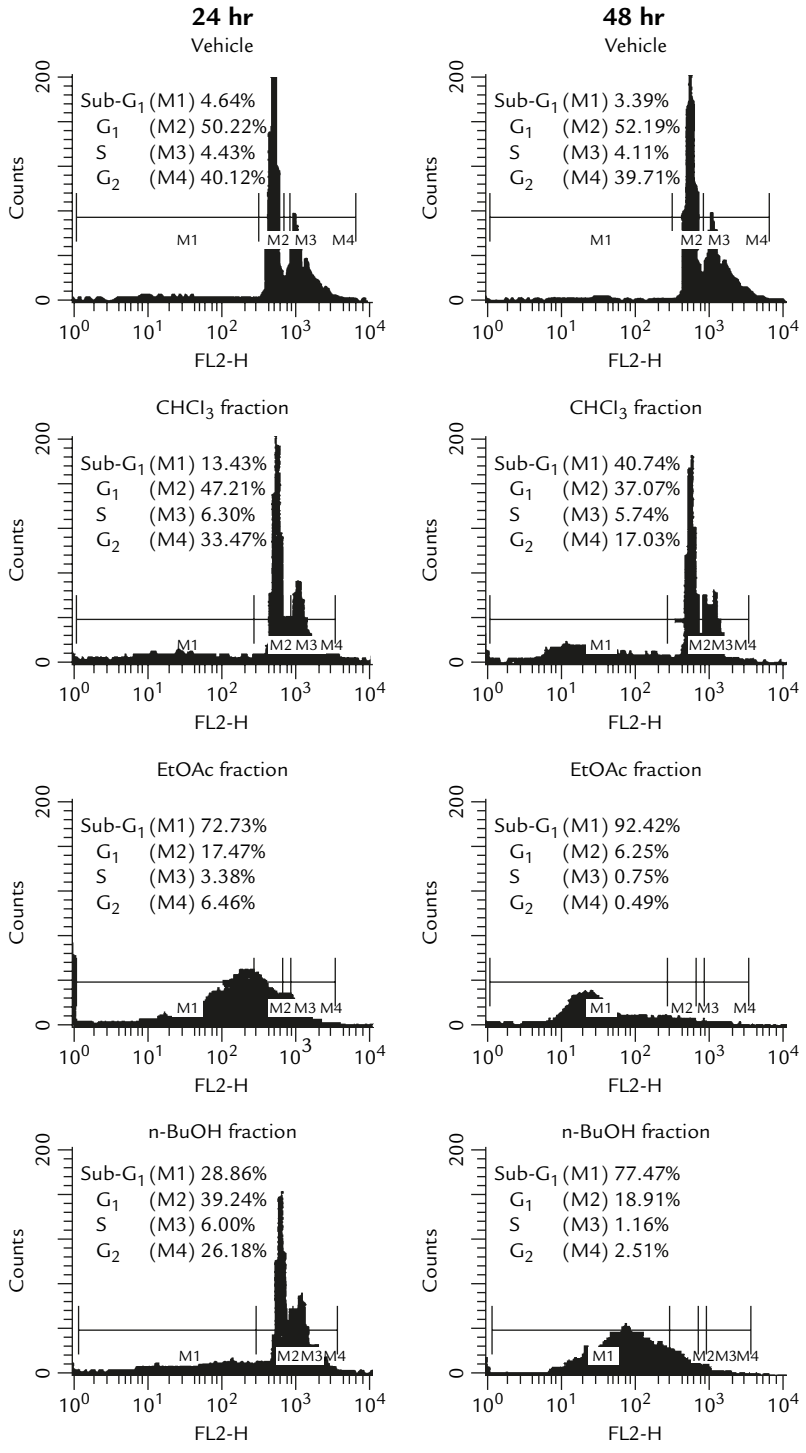


**Figure 4.** Cell cycle analysis of NIH3T3 cells treated with *Sauropus androgynus* (SA) extract. Cells were stained with propidium iodide after 24 or 48 hours' exposure to 300 μg/mL of DMSO, $CHCl_3$, EtOAc and n-BuOH fractions of SA extract and analyzed by flow cytometry. Distribution of vehicle or SA fraction treated cells are shown in the DNA histogram. Cell populations in different phases of cell cycle progression were gated by cell quest. Percentage of apoptotic cells was measured as sub-$G_1$ content of the histogram.

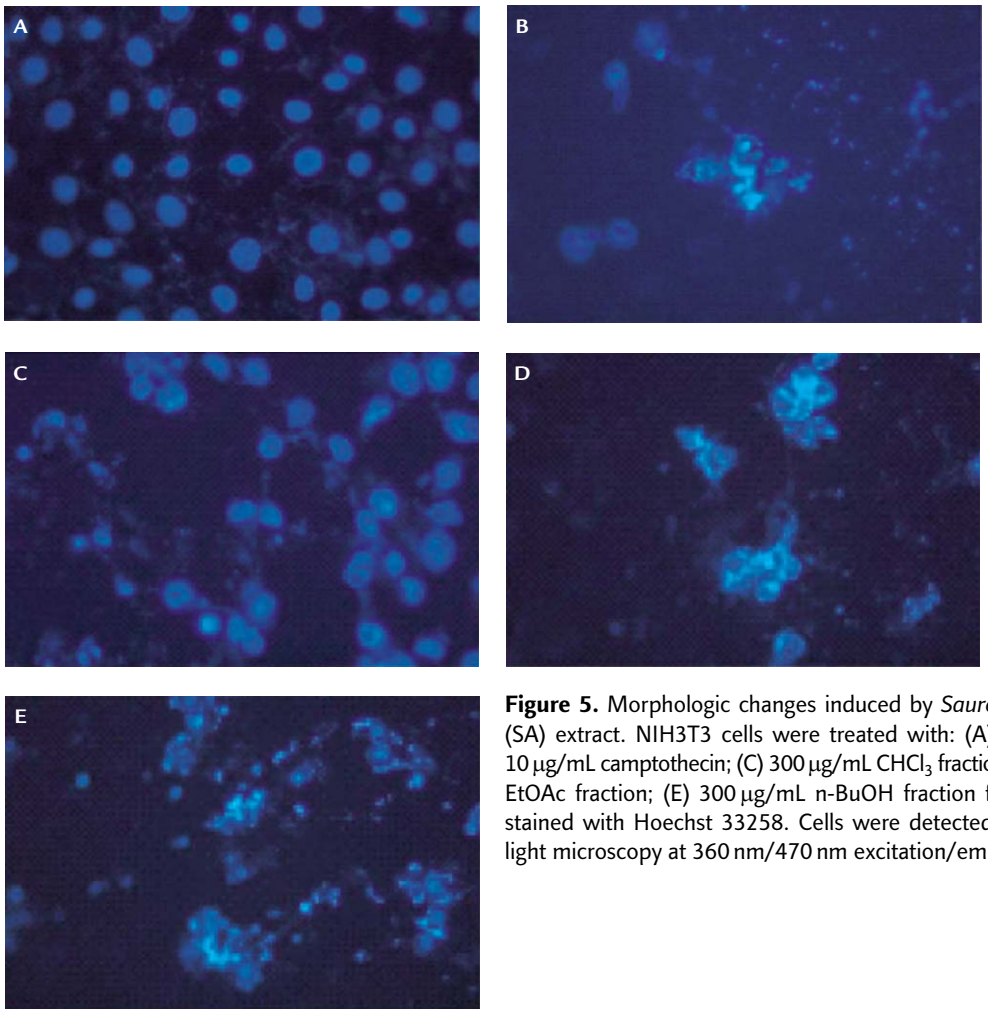


**Figure 5.** Morphologic changes induced by *Sauropus androgynus* (SA) extract. NIH3T3 cells were treated with: (A) 1% DMSO; (B) 10 μg/mL camptothecin; (C) 300 μg/mL $CHCl_3$ fraction; (D) 300 μg/mL EtOAc fraction; (E) 300 μg/mL n-BuOH fraction for 48 hours and stained with Hoechst 33258. Cells were detected by fluorescence light microscopy at 360 nm/470 nm excitation/emission (400×).

were stained with a DNA-specific fluorochrome. When cells were treated with EtOAc and n-BuOH fractions for up to 48 hours, there was a marked increase in PI fluorescence in the sub-$G_1$ area of the histogram, suggesting the induction of large amounts of DNA fragmentation.

The ratio of $G_1$ population in cell cycle progression increased when cells were treated with $CHCl_3$, EtOAc or n-BuOH fractions of SA extract for 48 hours. It may be caused by $G_1$ arrest or more cell death at the S and $G_2$/M phase. Flow cytometric analysis demonstrated the comparatively toxic activity of EtOAc fraction among three fractions in NIH3T3 cells. These results of FACS analysis are consistent with the levels of growth inhibition. However, it does not answer the cause of cell death through apoptosis or necrosis.

### *Modes of cell death in response to different fractions of SA extract*

NIH3T3 cells were cultured in 4% DMEM medium. Adding SA fractions led to sequentially morphologic changes. Typical condensation of the nucleus and chromatin appeared after cells were treated with camptothecin 10 μg/mL for 48 hours as a reference. Condensed DNA was observed when cells were treated with EtOAc and n-BuOH fractions of 300 μg/mL (Figures 5D and 5E). Treatment with $CHCl_3$ fraction of 300 μg/mL exhibited less nuclear condensation than treatment with the other two fractions (Figure 5C). Owing to blue spots occasionally observed in the cytoplasm of cells treated with SA fractions, we cannot exclude the possibility of contamination like mycoplasma and changes in cell susceptibility to SA fractions at this point. However, it at least shows

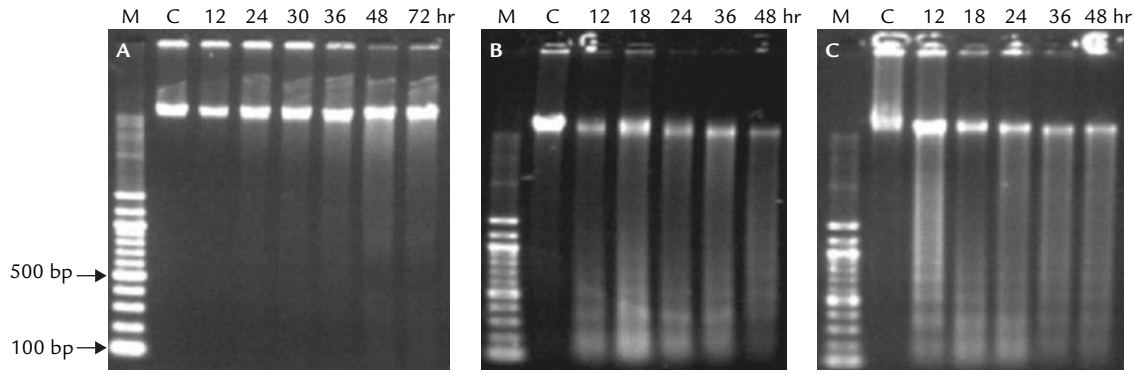


**Figure 6.** DNA ladders were analyzed by agarose gel electrophoresis. Cells were treated with $CHCl_3$ fraction of 300 μg/mL for 0–72 hours. (A) DNA smearing was detected from 24 to 72 hours. DNA extracts of cells treated with 300 μg/mL of (B) EtOAc fraction or (C) n-BuOH fraction were analyzed in parallel. DNA fragmentation was detected from 12 to 48 hours.

that EtOAc and n-BuOH fractions may induce an apoptosis-related pathway, resulting in NIH3T3 cell death.

### *Induction of apoptosis by EtOAc and n-BuOH fractions*

Caspase-activated DNase (CAD) is the major endonuclease during apoptosis to target internucleosomal DNA, causing extensive DNA fragmentation. Physiologic cell death is characterized by apoptotic morphology, including chromatin condensation, membrane blebbing, internucleosomal degradation of DNA and apoptotic body formation. In each case of nucleosomal DNA ladders, typical apoptosis was visible on agarose gels after staining with ethidium bromide. In the treatment of NIH3T3 cells with $CHCl_3$, EtOAc and n-BuOH fractions of 300 μg/mL for 0–72 hours, the genomic DNA was subjected to agarose gel electrophoresis. A clear DNA fragmentation ladder was observed in the lanes of EtOAc and n-BuOH fraction-treated cells (Figures 6B and 6C). This indicates that EtOAc and n-BuOH fractions induce genomic digestion over time. In contrast, cells treated with $CHCl_3$ fraction for 0–72 hours did not present internucleosomal DNA fragmentation (Figure 6A). The level of internucleosomal DNA fragmentation induced by EtOAc fraction was consistent with the most potent cytotoxicity of EtOAc fraction among the three fractions of SA extract.

### *Distinguishing apoptosis from necrosis induced by SA fractions in NIH3T3 cells*

Viable cells maintain an asymmetric distribution of different phospholipids between the inner and outer leaflets of the membrane. Annexin V interacts specifically with phosphatidyl serine and is used for detection of apoptosis by targeting for the loss of membrane asymmetry. PI has been displayed as binding strongly to DNA double helix. Apoptosis was observed by treating with fluorescein isothiocyanate (FITC)-labeled annexin V, and necrosis was detected by dye exclusion of PI. To quantify the level of induction in the annexin V-positive apoptotic and PI-positive necrotic cells, flow cytometric analysis was applied using a single cell suspension preparation method. Flow cytometric analysis of annexin V and PI labeling was used to differentiate apoptosis from necrosis in SA fraction-treated NIH3T3 cells. The cytograms in Figures 7A–D show the bivariate annexin V/PI analysis of the untreated cell suspension in comparison to the cells treated with partially purified fractions of SA extract (Figures 7E–7H). Vital cells are negative for both annexin V and PI, located at LL (lower left); apoptotic cells are annexin V positive and PI negative, scattering to LR (lower right); necrotic cells are annexin V negative and PI positive, scattering to UL (upper left); while dead cells are positive for both annexin V and PI, spreading in UR (upper right). After 48 hours of exposure

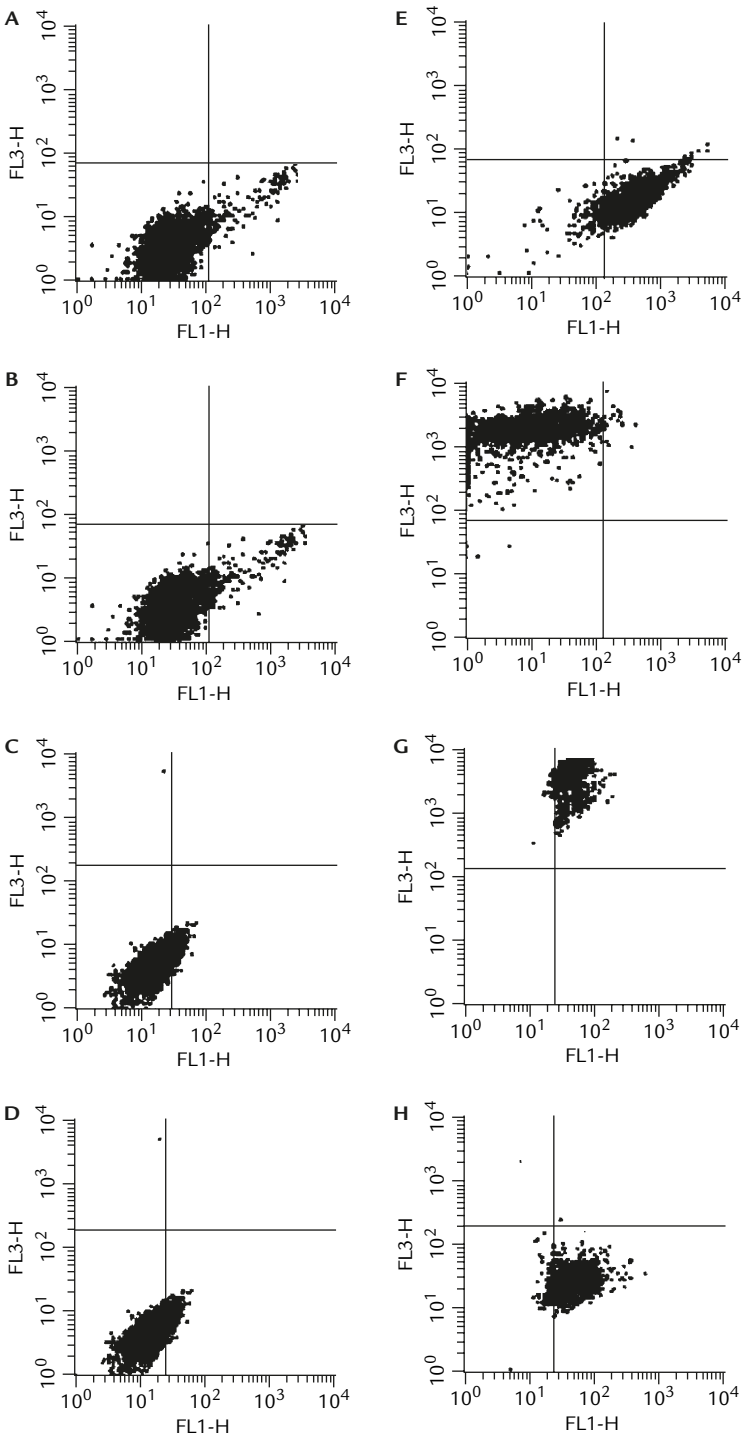


**Figure 7.** Bivariate dot plot of NIH3T3 cells treated with *Sauropus androgynus* (SA) fractions. Cells were treated with: (A–D) DMSO as control; (E) 10 μg/mL camptothecin; (F) 300 μg/mL $CHCl_3$ fraction; (G) 300 μg/mL EtOAc fraction; (H) 300 μg/mL n-BuOH fraction for 48 hours, followed by annexin V–propidium iodide double staining. Distribution of apoptotic, necrotic and vital cells was analyzed by FACScan flow cytometry.

to camptothecin, the number of apoptotic cells dramatically increased from 3% to 89% (Figure 7E). When cells were treated with the $CHCl_3$ fraction for 48 hours, 99% of cells were distributed over the UL area (Figure 7F). When cells were exposed to the EtOAc fraction, most cells scattered to the UR area (Figure 7G), whereas most n-BuOH fraction-treated cells spread to the LR area (Figure 7H). Bivariate analysis of the cytogram is applicable to differentiate and quantify necrosis and apoptosis occurring in cells treated with different fractions of SA extract.

## Discussion

Since most studies of SA have been focused on pathologic changes in the respiratory tract and lung tissue,[6,7,9,31] the cytotoxic mechanism of SA remains unclear. We therefore investigated the cytotoxicity caused by SA extract *in vitro* in the present study. NIH3T3 fibroblast cells, usually displaying highly diverse adhesion properties, were employed to examine if necrosis or apoptosis occurred at the cellular level in the presence of the fractionized SA extract. Several studies have investigated the role of airway epithelial tight junctions in the development of chronic disease.[32] NIH3T3 cells are originated from mouse embryonic fibroblastic cells localized at the cell cortex and adhesion regions,[33] and can provide an *in vitro* study model.

We have examined the chemical properties of SA extract, and found that SA extract is unstable under long-term storage. More than 50% of the SA extract decomposed with time at room temperature using TLC analysis, consistent with decreased cytotoxicity in NIH3T3 cells. Meanwhile, we did not detect the existence of papaverine constituent in SA extract through high-performance liquid chromatography analysis (data not shown), although there have been reports of a high level of papaverine in SA.[2,3] On the other hand, SA has been reported to contain three flavonol glucosides in BuOH-soluble EtOH extract, including two flavonol diosides identified as 3-*O*-β-D-glucosyl-7-*O*-α-L-rhamnosyl-kaempferol and 3-*O*-β-D-glucosyl-(1 → 6)-β-D-glucosyl-kaempferol, and a rare flavonol trioside 3-*O*-β-D-glucosyl-(1 → 6)-β-D-glucosyl-7-*O*-α-L-rhamnosyl-kaempferol.[5] The flavonoid 3-*O*-β-D-glucosyl-(1 → 6)-β-D-glucosyl-kaempferol presents a reduction of body weight gain in Wistar rats.[34]

Three parts of SA extract, including $CHCl_3$, EtOAc and n-BuOH fractions, apparently display distinguishable cytotoxic effects. The $CHCl_3$ fraction induces NIH3T3 cell necrosis, implying that the outbreak of bronchiolitis obliterans evoked by SA ingestion might be caused partly by severe respiratory cell necrosis. After taking raw SA, some people developed respiratory distress symptoms due to an increased expression of interleukins in bronchoalveolar lavage fluid, as well as increased concentration of tumor necrosis factor-alpha (TNF-α), one of the fibrogenic cytokines,[35] in the sera of patients with SA-associated constrictive bronchiolitis obliterans.[7,8] Segmental necrosis of small bronchi has been reported in the airways of SA-associated lung disease[11] and a spectrum of inflammatory fibrotic changes in the bronchioles has also been observed. Some chemical-treated cells induce oxidative stress to produce reactive oxygen species, resulting in fragmentation of DNA.[36] SA extract is a complicated mixture containing high levels of oxidants that may be one of the etiologic factors in the development of SA-induced bronchiolitis obliterans[37] and chronic obstructive pulmonary disease.[11] Local tissue damage may be amplified by subsequent release of intracellular enzymes and lysosomal content, resulting in the recruitment of inflammatory cells to the site of injury, causing further necrosis of the surrounding tissues. Similar events were observed in SA extract-treated NIH3T3 cells where chromatin dysfunctions such as single- or double-stranded DNA fragmentation occurred, perhaps leading to cell death through necrosis or apoptosis. Necrotic cells have fewer DNA strand breaks, and in some instances of necrosis, DNA fragmentation may be indistinguishable from apoptotic cells.[28] When ATP is depleted, apoptosis stops progressing, and the proapoptotic signals turn out to induce necrotic cell death. It is a so called switch from necrosis to apoptosis mediated by ATP supply.[20] Glucose depletion affects both the production of ATP by glycolysis and the supply of substrates to the mitochondria, causing segmental ischemic necrosis of the bronchi.[11]

Cells treated with $CHCl_3$ fraction exhibit not only random DNA fragmentation but also a series of cell death markers such as slight elevation of cell cycle sub-$G_1$ population, morphologic changes and DNA smearing. In fact, morphologically necrotic changes occur in the cells treated with either $CHCl_3$ or EtOAc fraction. Bursting of the plasma membrane abruptly ends the metastable period and may cause onset of necrotic cell death in NIH3T3 cells exposed to $CHCl_3$ or EtOAc fraction.

In contrast, NIH3T3 cells exposed to n-BuOH fraction has led to typical apoptotic chromatin condensation and nuclear fragmentation, detected by Hoechst staining.

Flow cytometric analysis demonstrates that NIH3T3 cells are largely inhibited from entering $G_0$–$G_1$ when cells are treated with EtOAc and n-BuOH fractions, according to up to 77–92% cell population undergoing cell death in sub-$G_1$. Certain unclear oxidative ingredients of SA extract might be involved in cell growth inhibition. Incomplete DNA repair in conjunction with increased intracellular oxidative stress reduced intracellular GSH levels and increased cytotoxicity.[38] Large amount of cell death gives rise to complete derangement of cell cycle progression. The higher percentage of the $G_1$ phase cells may be caused by $G_1$ arrest or more cell death at the S and $G_2$/M phase after treatment with EtOAc or n-BuOH fraction for 48 hours. Instead, $CHCl_3$ fraction treatment has only a small population of fragmented DNA accumulation in the sub-$G_1$ phase. It is again revealing the distinguished mechanism induced by $CHCl_3$ fraction in NIH3T3 cells, perhaps in part associating with ischemic necrosis of respiratory tract tissues in patients receiving raw SA. Bivariate annexin V/PI analysis of the cytogram in our experiments is the most important evidence to claim that either necrosis or apoptosis induced in NIH3T3 cells depends on the treatment with different fractions of SA extract. In previous studies, only necrosis-related pathologic changes were reported in cartilage, bronchial glands and smooth muscle cells.[11] However, apoptosis was clearly observed in cells treated with the n-BuOH fraction *in vitro*. The intermediate fraction, EtOAc fraction, containing the activity in between, presents both necrosis and apoptosis in the *in vitro* study. To understand the molecular basis of necrosis and apoptosis evoked by various SA fractions, further studies are required. In addition, searching for the unknown constituents in SA extract responsible for weight loss will be very interesting. If the effective constituents can be separated from the toxic ones, it would be of clinical value in anti-obesity in the future.

## Acknowledgments

This work was supported by a grant (NSC 89-2314-B-002-054) from the National Science Council. The authors thank Dr Shoei-Sheng Lee for helpful discussions and assistance with separation of SA extract.

## References

1. Martin FW, Ruberte RM. Techniques and plants for the topical subsistence farm. *United States Department of Agriculture*, 1980:56.
2. Bender AE, Ismail KS. Nutritive value and toxicity of *Sauropus androgynous*. *Proc Nutr Soc* 1973;32:79A–80A.
3. Padmavathi P, Rao MP. Nutritive value of *Sauropus androgynus* leaves. *Plant Foods Hum Nutr* 1990;40: 107–13.
4. Kanchanapoom T, Chumsri P, Kasai R, et al. Lignan and megastigmane glycosides from *Sauropus androgynus*. *Phytochem* 2003;63:985–8.
5. Wang PH, Lee SS. Active chemical constituents from *Sauropus androgynus*. *J Chin Chem Soc* 1997;44:145–9.
6. Wang JS, Tseng HH, Lai RS, et al. *Sauropus androgynus*-constrictive obliterative bronchitis/bronchiolitis—histopathological study of pneumonectomy and biopsy specimens with emphasis on the inflammatory process and disease progression. *Histopathology* 2000;37:402–10.
7. Lai RS, Chiang AA, Wu MT, et al. Outbreak of bronchiolitis obliterans associated with consumption of *Sauropus androgynus* in Taiwan. *Lancet* 1996;348:83–5.
8. Lai RS, Wang JS, Wu MT, Hsu HK. Lung transplantation in bronchiolitis obliterans associated with vegetable consumption. *Lancet* 1998;352:117–8.
9. Hsiue TR, Guo YL, Chen KW, et al. Dose-response relationship and irreversible obstructive ventilatory defect in patients with consumption of *Sauropus androgynus*. *Chest* 1998;113:71–6.
10. Chen CW, Hsiue TR, Chen KW, et al. Increased IL-5 and IL-10 transcription in bronchial cells after *Sauropus androgynus* ingestion. *J Formos Med Assoc* 1996;95:699–702.
11. Chang YL, Yao YT, Wang NS, Lee YC. Segmental necrosis of small bronchi after prolonged intakes of *Sauropus androgynus* in Taiwan. *Am J Respir Crit Care Med* 1998; 157:594–8.
12. Majno G, Joris I. Apoptosis, oncosis, and necrosis. An overview of cell death. *Am J Pathol* 1995;146:3–15.
13. Thornberry NA, Lazebnik Y. Caspases: enemies within. *Science* 1998;281:1312–6.
14. Kerr JF, Wyllie AH, Currie AR. Apoptosis: a basic biological phenomenon with wide-ranging implications in tissue kinetics. *Br J Cancer* 1972;26:239–57.

15. Leist M, Gantner F, Jilg S, Wendel A. Activation of the 55 kDa TNF receptor is necessary and sufficient for TNF-induced liver failure, hepatocyte apoptosis, and nitrite release. *J Immunol* 1995;154:1307–16.
16. Nicotera P, Melino G. Regulation of the apoptosis–necrosis switch. *Oncogene* 2004;23:2757–65.
17. Ferrari D, Stepczynska A, Los M, et al. Differential regulation and ATP requirement for caspases-8 and caspases-3 activation. *J Exp Med* 1998;188:979–84.
18. Los M, Mozoluk M, Ferrari D, et al. Activation and caspases-mediated inhibition of PARP: a molecular switch between fibroblast necrosis and apoptosis in death receptor signaling. *Mol Biol Cell* 2002;13:978–88.
19. Ha HC, Snyder SH. Poly (ADP-ribose) polymerase is a mediator of necrotic cell death by ATP depletion. *Proc Natl Acad Sci U S A* 1999;96:13978–82.
20. Kim JS, Qian T, Lemasters JJ. Mitochondrial permeability transition in the switch from necrotic to apoptotic cell death in ischemic rat hepatocytes. *Gastroenterology* 2003;124: 494–503.
21. Yoshioka A, Yamaya Y, Saiki S, et al. Non-N-methyl-D-aspartate glutamate receptors mediate oxygen—glucose deprivation-induced oligodendroglial injury. *Brain Res* 2000;854:207–15.
22. Lizard G, Monier S, Cordelet C, et al. Characterization and comparison of the mode of cell death, apoptosis versus necrosis, induced by 7beta-hydroxycholesterol and 7-ketocholesterol in the cells of the vascular wall. *Arterioscler Thromb Vasc Biol* 1999;19:1190–200.
23. Oppenheim RW, Flavell RA, Vinsant S, et al. Programmed cell death of developing mammalian neurons after genetic deletion of caspases. *J Neurosci* 2001;21:4752–60.
24. Gorczyca W, Melamed MR, Darzynkiewicz Z. Analysis of apoptosis by flow cytometry. *Methods Mol Biol* 1998; 91:217–38.
25. Steck K, McDonnell T, Sneige N, el-Naggar A. Flow cytometric analysis of apoptosis and bcl-2 in primary breast carcinomas: clinical and biological implications. *Cytometry* 1996;24:116–22.
26. Mosmann T. Rapid colorimetric assay for cellular growth and survival: application to proliferation and cytotoxicity assays. *J Immunol Methods* 1983;65:55–63.
27. Battaglia M, Pozzi D, Grimaldi S, Parasassi T. Hoechst 33258 staining for detecting mycoplasma contamination in cell cultures: a method for reducing fluorescence photobleaching. *Biotech Histochem* 1994;69:152–6.
28. Gorczyca W. Cytometric analyses to distinguish death processes. *Endocr Relat Cancer* 1999;6:17–9.
29. Vermes I, Haanen C, Steffens-Nakken H, Reutelingsperger C. A novel assay for apoptosis. Flow cytometric detection of phosphatidylserine expression on early apoptotic cells using fluorescein labelled annexin V. *J Immunol Methods* 1995;184:39–51.
30. Del BG, Darzynkiewicz Z, Degraef C, et al. Comparison of methods based on annexin-V binding, DNA content or TUNEL for evaluating cell death in HL-60 and adherent MCF-7 cells. *Cell Prolif* 1999;32:25–37.
31. Lin TJ, Lu CC, Chen KW, Deng JF. Outbreak of obstructive ventilatory impairment associated with consumption of *Sauropus androgynus* vegetable. *J Toxicol Clin Toxicol* 1996;34:1–8.
32. Devalia JL, Godfrey RW, Sapsford RJ, et al. No effect of histamine on human bronchial epithelial cell permeability and tight junctional integrity *in vitro*. *Eur Respir J* 1994; 7:1958–65.
33. Paddenberg R, Loos S, Schoneberger HJ, et al. Serum withdrawal induces a redistribution of intracellular gelsolin towards F-actin in NIH 3T3 fibroblasts preceding apoptotic cell death. *Eur J Cell Biol* 2001;80:366–78.
34. Yu SF, Shun CT, Chen TM, Chen YH. 3-O-β-D-glucosyl-(1 → 6)-β-D-glucosyl-kaempferol isolated from *Sauropus androgenus* reduces body weight gain in Wistar rats. *Biol Pharm Bull* 2006;29:2510–3.
35. Piguet PF, Grau GE, Vassalli P. Subcutaneous perfusion of tumor necrosis factor induces local proliferation of fibroblasts, capillaries, and epidermal cells, or massive tissue necrosis. *Am J Pathol* 1990;136:103–10.
36. Higuchi Y. Chromosomal DNA fragmentation in apoptosis and necrosis induced by oxidative stress. *Biochem Pharmacol* 2003;66:1527–35.
37. Luh SP, Lee YC, Chang YL, et al. Lung transplantation for patients with end-stage *Sauropus androgynus*-induced bronchiolitis obliterans (SABO) syndrome. *Clin Transplant* 1999;13:496–503.
38. Bijur GN, Ariza ME, Hitchcock CL, Williams MV. Antimutagenic and promutagenic activity of ascorbic acid during oxidative stress. *Environ Mol Mutagen* 1997;30: 339–45.